Accepted Manuscript

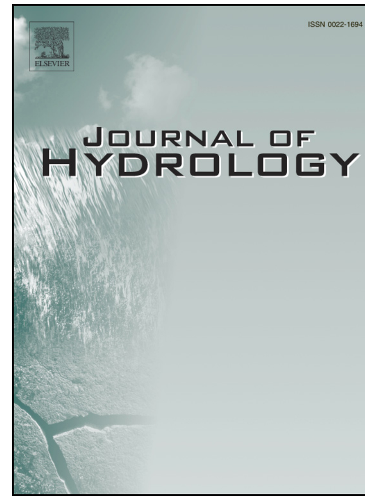

Temporal variability of karst aquifer response time established by the sliding-windows cross-correlation method

Célestine Delbart, Danièle Valdés-Lao, Florent Barbecot, Antoine Tognelli, Patrick Richon, Laurent Couchoux

PII: S0022-1694(14)00105-X
DOI: http://dx.doi.org/10.1016/j.jhydrol.2014.02.008
Reference: HYDROL 19399

To appear in: *Journal of Hydrology*

Received Date: 5 November 2013
Revised Date: 22 January 2014
Accepted Date: 1 February 2014

Please cite this article as: Delbart, C., Valdés-Lao, D., Barbecot, F., Tognelli, A., Richon, P., Couchoux, L., Temporal variability of karst aquifer response time established by the sliding-windows cross-correlation method, *Journal of Hydrology* (2014), doi: http://dx.doi.org/10.1016/j.jhydrol.2014.02.008

Temporal variability of karst aquifer response time established by the sliding-windows cross-correlation method

Revised version of HYDROL15869

Célestine Delbart [1]*, Danièle Valdés-Lao[2], Florent Barbecot[3], Antoine Tognelli[1], Patrick Richon[1], Laurent Couchoux[4]

[1]CEA, DAM, DIF, F-91297 Arpajon, France. UMR IDES 8148, Université Paris-Sud-CNRS, France

[2]UPMC Univ. Paris 06, UMR 7619 Sisyphe, Case 105, 4 place Jussieu, F-75005 Paris, France

[3]GEOTOP, Université du Quebec à Montréal, Montréal, Québec H3C 3P8, Canada

[4] CEA, DAM, Valduc, 21120 Is-sur-Tille, France

* Corresponding author. Tel :33(0)1.69.15.67.53; Fax : Fax: +33-(0)1 69 15 49 05 . E-mail address: celestine.delbart@gmail.com; Affiliation details : CEA, DAM, DIF, F-91297 Arpajon, France and UMR IDES 8148, Université Paris-Sud-CNRS, France

Abstract

We study the temporal variability of water transfer through the infiltration zone of a karst aquifer by estimating the impulse response of the system using cross-correlogram analyses between rainfall and piezometric level time series. We apply a sliding-window cross-correlation method, which calculates cross-correlograms on partially superposed short time series windows. We apply this method for rainfall and piezometric level time series at six boreholes in a fractured karstic aquifer located in Burgundy, France. Based on cross-correlogram functions, we obtain a time series of response time. At most of the boreholes, the cross-correlation functions change over time, and the response times vary seasonally, being shorter during the summer. This unusual structure can be partly explained by the seasonal variability in rainfall intensity, which is higher during the summer (May to September), inducing the seasonal behaviour of the epikarst. During the summer, when rainfall intensity is higher, the epikarst is more easily and quickly saturated. This induces an increase in lateral water transfer within the epikarst and an increase in concentrated fast flows. We also show that the response time seems to tend towards a limit which represents the maximum saturation of the epikarst.

Keywords: Karst aquifer; time series analysis; sliding-windows cross-correlation; response time.

1. Introduction

Karst aquifers are usually characterised by heterogeneous physical properties and multiple transfer velocities due to the presence of open conduits created by the dissolution of calcite (Aquilina et al., 2005; White, 2002). However, regardless of the degree of karstification and the extent of the conduit network, aquifers present a distribution of transfer velocity from low and diffuse flow to fast and conduit flow (Atkinson, 1977; Larocque et al., 1998; White, 1969).

Numerous methods have been proposed to decipher and describe the functioning of karst aquifers. Classical techniques include geologic and geomorphologic observations, pumping tests (McConnell, 1993; Thrailkill, 1988), tracer tests (Goldscheider et al., 2008; Käss, 1998; Kogovsek and Petric, 2003; Smart, 1988), analysis of chemographs of major chemicals, stable isotopes and carbon-13 (Aquilina et al., 2005; Emblanch et al., 2003)), analysis of recession curves (Atkinson, 1977; Birk and Hergarten, 2010; Kovács and Perrochet, 2008; Mangin, 1984; Milanovic, 1981; Shevenell, 1996), spectral and correlation analysis, wavelet analysis (Angelini, 1997; Jukić and Denić-Jukić, 2011; Labat et al., 2000; Larocque, 1997; Mangin, 1975; Panagopoulos and Lambrakis, 2006; Rahnemaei et al., 2005), geophysical investigation (Jacob et al., 2008), reservoir models (Fleury et al., 2007; Geyer et al., 2008; Jukić and Denić-Jukić, 2009; Tritz et al., 2011), spring hydrograph models from spectral analysis (Jukić and Denić-Jukić, 2004) and numerical and physical models (Dreybrodt, 1996; Dreybrodt et al., 2005; Eisenlohr et al., 1997; Scanlon et al., 2003).

The karst investigations previously presented have defined a basic conceptual model of the karst system in two parts: the infiltration, or unsaturated, zone and the saturated, or phreatic, zone.

The infiltration zone consists of two parts: the epikarst and the transition zone. The epikarst is the uppermost zone of carbonate rocks that are particularly corroded or fractured, due to stress release, weathering and dissolution (Klimchouk, 2004). The contrast in permeability between the epikarst and the transition zone gives the epikarst the ability to regulate water infiltration and storage (Aquilina et al., 2005; Bakalowicz, 2010; Mangin, 1975; Perrin et al., 2003). The infiltration from the epikarst towards the transition zone is divided into two components: a slow seepage from the base of the epikarst and a concentrated flow through high conductivity conduits. The lateral component flow is significant in the epikarst, allowing the water to converge towards vertical fissures (Perrin et al., 2003). The transition zone is the zone between the epikarst and the saturated zone. The flow is essentially vertical. Two types of water flow coexist: slow flow in small fractures and quick flow in large conduits.

The saturated zone can be divided into two subparts: conduits that mostly drain water towards the karst spring and a low permeability volume where water is stored. The storage capacity of the saturated zone is still in question, and several models have been proposed: a model in which water is stored in matrices or fractures (Drogue, 1974; Mudry, 1990) and a model in which water is stored in karst voids (Mangin, 1975).

The goal of this project is to characterise the functioning of a karst aquifer located in Burgundy, France, to protect water resources from accidental pollution. In this paper, we analyse the seasonal variability of the impulse response of this aquifer. We determine the impulse response of the karst aquifer from cross-correlation analyses between rainfall and piezometric levels and adapt this method to study the variability of the impulse response over time with the application of cross-correlation analyses over three-month periods by sliding windows.

Correlation and spectral analyses are methods based on statistical tools developed principally by Jenkins and Watts (1968) and Box et al. (1994) and adapted to karst systems by Mangin (1975). A karst aquifer can be viewed as a filter transforming an input signal into an output signal by a transfer function (Mangin, 1984; Mathevet et al., 2004; Walliser, 1977). Once defined, this function can be interpreted to define the functioning, organisation and structure of karst aquifers.

Two types of correlation analyses are typically used: auto-correlation and cross-correlation. The first analysis characterises the individual structure of the time-series and its linear dependency over a period of time. The second analysis characterises the link between the input and output signals and usually considers rainfall as an input signal and discharge at a spring as an output signal (Mangin, 1975). This cross-correlation is the picture of the impulse response of a karst system, if the rainfall can be considered random. From this analysis, the average response time of the aquifer to a rainfall event can be computed.

Historically, in karst aquifers, spectral and correlative analyses are conducted between precipitation and spring discharge, giving information on the entire system. Some authors use these methods for other types of time series. From piezometric levels, they obtain information at several locations of the aquifer to evaluate the impact of unsaturated or epikarstic zones. Some authors propose to adapt this method to study the mass transfer in aquifers using conductivity (Bailly-Comte et al., 2011; Larocque et al., 1998), turbidity (Amraoui et al., 2003; Bailly-Comte et al., 2011; Bouchaou et al., 2002; Massei et al., 2006) and temperature (Bailly-Comte et al., 2011) time series. Some hydrogeologic processes are underlined by a temporal lag between piezometric and geochemical variation, such as surface water arrival (Hanin, 2010).

The size of time series can vary depending on the goal of the study. Previous studies on long periods (pluri-annual time series) have given global information on the system (Andreo et al., 2006; Larocque et al., 1998; Pulido-Bosch et al., 1995; Rahnemaei et al., 2005). Some authors compared several hydrological cycles and analysed the variability of the impulse response depending on the cumulative precipitation (Hanin, 2010; Larocque et al., 1998). Lee et al. (2006) chose three-month periods, and Larocque et al. (1998) divided the hydrological year along the low and high water table periods. Both authors established that the seasonal variability of the impulse response provides a picture of the seasonal variations of the water table (variability of unsaturated zone thickness, variability of network saturation). A method to study the temporal variation of properties within the aquifer was proposed by Bailly-Comte et al. (2011). They used a sliding cross-correlogram method between temperature and specific conductivity time series and established that residence time variations are connected with flow (high and low flow).

In this paper, we analyse the temporal variability of the impulse response using the sliding cross-correlogram method between rainfall and piezometric level time series to interpret temporal variability in seasonal hydrological processes.

First, we discuss the study area, data acquisition and the sliding cross-correlation method. We then apply this method to study the temporal variation of the response time and discuss the implications for understanding the physical mechanisms involved in this karst aquifer.

2. Study area

The study area is located in Burgundy, 30 km to the northwest of Dijon in eastern France (Fig. 1). The study zone is on the catchment of the Douix de Léry River (Fig. 1). This area is approximately 40 km^2, with a maximum altitude of 501 m NGF and a minimum altitude of 336 m NGF. The land in this catchment is composed of forest (82.5% of total surface), agricultural land (13% of total surface) and urban area (4.5% of total surface). The urban area, located on the north of the study site (Fig. 1), is principally composed of parking lots, roads and buildings, which cause runoff and some preferential zones of infiltration downstream of the urban area.

The climate is continental. The average atmospheric temperature is approximately 9.7°C, with a maximum temperature in June, July and August, and the cumulative rainfall by hydrological cycle ranges between 689 mm and 1214 mm, with an average of 955 mm (1992-

2012, Météo-France data at Saint Martin du Mont station, located 18 km south-southwest of the study site centre).

From June 2007 to October 2012 (the period of study), the cumulative rainfall does not present significant inter-annual changes. The average cumulative rainfall in a hydrological cycle is 916 mm, with a standard deviation of 55 mm. The rainiest hydrological cycle is October 2011-October 2012, with a cumulative rainfall of 978 mm, close to the average over the 1992-2012 period. The least rainy hydrological cycle is October 2010-October 2011, with 832 mm of cumulative rainfall, 13% less than the average values of the last twenty years. The monthly cumulative rainfall is not seasonally distributed. The average intensity of rainfall, in mm/h, which is defined as the average intensity of rainfall in mm/h without taking into account the intensities equal to zero, varies seasonally. The intensity of rainfall is highest in July and August and lowest in January and February (Fig. 2).

The geologic section is composed of tabular Jurassic limestones interspersed by marls, allowing the development of two superposed aquifers. In this publication, only the upper one will be monitored and studied. The subsurface is composed of several layers of limestone: Comblanchien, oolitic and oncholite limestones underlain by marls of the Upper Bajocian formation (Fig. 1). The thickness of the limestone layer varies from 0 m (spring location) to 70 m, depending on the location. The studied aquifer is located in the oncholite limestone layer.

The limestones are characterised by three types of porosity. Matrix porosity is related to the internal structure of the limestone, fracture porosity reflects the tectonic history of the region, and the conduit porosity is due to the dissolution of the calcite. Primary porosity has been studied in the laboratory. Permeability and porosity measurements were measured using a non-steady-state air permeameter and the mercury intrusion method, respectively, in several limestones. Primary porosity is low, with a maximum of 16% in the oolitic limestone. From the marls to the top of oolitic limestone, the porosity, the permeability and the pore size increase. The total porosity varies from 4 to 16%, the effective porosity from 2 to 7% and the average hydraulic conductivity of limestone is 4.10^{-8} $m \cdot s^{-1}$. A higher density of stylolites is noticed in the oncolites limestone layer, increasing the permeability of the limestone. In the Comblanchien limestone, the total porosity is approximately 5%, but the effective porosity and permeability approach zero.

The fracture porosity is apparent in the field or in rock cores. This porosity is characterised by high heterogeneity, in either size or density. The fracture openings vary from millimetre-scale up to 20 cm, with an average of 3 cm for 654 measured fractures. The average distance between two fractures is approximately 2 m.

The conduit porosity is linked to the dissolution of carbonate rock. In the field, some karst conduits have been observed; their size can be as large as a few metres (5 m). No underground cavities are known. Some artificial flow tracings have been done on the site, giving a modal velocity which varies from $2x10^{-4}$ to $6x10^{-3}$ $m.s^{-1}$.

The thickness of the soil is low and varies between 0.20 to 1.60 m. The soil surface characteristics were investigated in situ. We measured the hydraulic conductivity at saturation using a double-ring infiltrometer to be between $8x10^{-5}$ and $1x10^{-3}$ $m.s^{-1}$. We determined the hydraulic conductivity of near-saturated soils using tension disc infiltrometers and found that it varies between $4x10^{-5}$ and $1.4x10^{-4}$ $m.s^{-1}$. The high values of hydraulic conductivity induce a low runoff effect and a high ratio of vertical transport. The epikarst is located under the soil and is characterised by a high density of fractures compared with the carbonate located below. Its thickness varies from 5 to 10 m, depending on the location.

3. Data acquisition

We monitored the piezometric levels at six boreholes from June 2007 to September 2012, with an acquisition time interval of 1 h. The locations of the measurement stations are shown in Fig. 1, and key characteristics of each site are presented in Table 1 (altitude, dominant land use, unsaturated zone thickness). Piezometric levels are measured with Mini-Diver^{TM} probes compensated for atmospheric pressure using a barodiver (*Schlumberger Water Service).* The accuracy of the measurements are ±1 cm H_2O (borehole A1, C2, D1, D35, S3) and ±3 cm H_2O (borehole S3), depending on the amplitude of piezometric level variation. Due to minor technical problems, some of the time series of piezometric levels include data gaps (a maximum of 5% of the complete time series).

The rainfall time series was supplied by Météo-France at Saint Martin du Mont station, located 17.6 km from the S3 borehole. Precipitation was recorded hourly.

4. Auto-correlation, cross-correlation and sliding-window cross-correlation methods

4.1 Auto-correlations and cross-correlations

A short explanation of these statistical methods is presented below. Further demonstrations and theoretical analyses have been established by Box et al. (1994), Jenkins and Watts (1968) and Mangin (1984). The auto-correlation function of a time series quantifies the linear dependency of successive values over a time period and can be written as:

For k>0,

$$C(k) = \frac{1}{n}\sum_{t=1}^{n-k}(x_t - \bar{x})(x_{t+k} - \bar{x}) \quad \textbf{(1)}$$

$$r(k) = \frac{C(k)}{C(0)} \quad \textbf{(2)}$$

where r(k) is the auto-correlation function, C(k) is the correlogram, k is the time lag (k=0 to m), n is the length of the time series, x_t is the value of the studied variable at time t, and m is the cutting point (Box et al., 1994). The cutting point determines the interval in which the analysis is conducted. It is necessary that m ≤ n/3 to define C(k) for each k with the same number of data.

For a random variable, this function, r(k), decreases very quickly and reaches zero for short time lags. To compare the inertia of signal, Mangin (1984) defines the memory effect as the time lag required for the auto-correlation function to reach a predefined value, which is usually 0.2.

The cross-correlation function is used to establish relationships between the input and output time series and can be written as:

For k>0:

$$C_{xy}(k) = \frac{1}{n}\sum_{t=1}^{n-k}(x_t - \bar{x})(y_{t+k} - \bar{y}) \quad \textbf{(3)}$$

$$r_{xy}(k) = \frac{c_{xy(k)}}{\sigma_x \sigma_y} \quad \textbf{(4)}$$

where k is the time lag; n is the length of the time series; x_t and y_t are input and output time series, respectively; $r_{xy}(k)$ is the cross-correlation function; σ_x and σ_y are the standard deviations of the time series; and $C_{xy}(k)$ is the cross-correlogram (Box et al., 1994).

If the cross-correlogram function is not symmetrical and if $r_{xy}(k)$ shows maximum or minimum for a positive lag, the input signal influences the output signal. If the input time series is random, the cross-correlation function corresponds to the impulse response (Box et al., 1994).

The response time is the lag time that corresponds to the maximum of the cross-correlation function. The response time related to the cross-correlation between rainfall and discharge or piezometric level corresponds to the mean response time of the karst aquifer to a rainfall event (Mangin, 1984).

4.2 Sliding window cross-correlation method

To highlight the seasonal variability of the impulse response, we propose to adapt cross-correlation method. Using the sliding window cross-correlation method between rainfall and piezometric level allows us to study the temporal evolution of the relationship between the input and output time series.

The sliding-window cross-correlation method consists of slicing the input (precipitation) and the output (piezometric level) time series with partially superposed windows. For each window, the cross-correlogram function between rainfall and piezometric level is calculated, and the response time is determined (Fig. 3). We then obtain a time series of response time.

The length and lag of windows have to be chosen appropriately depending on the study (goal of study and frequency of events). Here, we slice the time series into "three-month periods" lagged by one-and-a-half months to show the presence of seasonal variability.

To be acceptable, a cross-correlation function has to be characterised by a significant correlation at the 95% confidence level, which means a correlation coefficient, r(k), superior to the standard error $\sim\frac{2}{N^{1/2}}$, where N is the number of values in the data set (Diggle, 1990; Lee et al., 2006).

The sliding window cross-correlation method requires a high frequency of rainfall events and reactive piezometric time series throughout the year.

5. Results

First, we present and analyse the time series of rainfall and piezometric level as a whole (2007-2012). Second, we apply the sliding window cross-correlogram method to study the temporal variability of the relationship between rainfall and water level.

5.1 Rainfall and piezometric level time series description

The monitoring in the field gives the piezometric level every hour at six boreholes for nearly six years (Fig. 4). The high-frequency variations in the piezometric level indicate that these six boreholes are reactive, meaning the piezometric level varies after a rainfall event throughout the year. The fast response time is probably partly due to the runoff and preferential zone of infiltration, linked to the urban area. Nevertheless, some boreholes located in forest areas are also characterised by short response times. A very fast transfer velocity in karst conduits with a low dependence on evapotranspiration could explain the short time response events throughout the year. The high frequency of recharge events allows us to apply the sliding window cross-correlogram method.

5.2 Application of the sliding-window cross-correlation method

The sliding-window cross-correlation method was performed between the rainfall and the piezometric level at six boreholes during the period of June 2007-September 2012 with three-month period windows and a lag of 1.5 months. We obtained 42 cross-correlogram functions.

The frequency of recharge events has to be enough for a three-month period because it influences estimates of cross-correlation functions between rainfall and spring discharge (Eisenlohr et al., 1997). At this site, there is an average of 17 rainfall events (rough count) over a three-month period, with a minimum of 11 and a maximum of 26. Furthermore, the input time series is supposed to be random to interpret the cross-correlation as the impulse response of the system. The rainfall auto-correlation is calculated for each three-month window. Most of the time, the rainfall auto-correlation functions decrease sharply for lag values close to zero. The maximum memory effect for an r(k) of 0.2 is 13 h, and the average memory effect is 4 h. Therefore, we consider rainfall to be approximately random for each window.

The application of the sliding cross-correlation on the studied period gives a maximum of 41 windows for each borehole. Due to the data gap in the time series, we obtain 39 to 41 cross-correlograms, depending on the borehole. Furthermore, we do not take into account windows when the correlation coefficient is not significant (less than 0.043; significant correlation at the 95% confidence level). We note that some cross-correlation functions present several peaks, which could highlight the existence of multiple flows within the aquifer

(Massei et al., 2006). However, the characterisation of multiple flows is beyond the scope of this study. Therefore, we focus on the fast transfer in the karst aquifer using only the first correlation peak.

At the end of this pre-treatment, the time series of the response time is composed of 32 to 41 values. The response time is not constant during the year (Fig. 5) but remains short, between 5 to 140 h (Table 2). For each borehole, we observe a high variability in response time. For example, the response times of the A1 borehole vary between 5 and 42 h, and those of the F7 borehole vary between 20 and 107 h. For the D1, D35, F7, C2 and A1 boreholes, the response time varies seasonally, with lower values during the summer (Fig. 5 and 6). This relationship is unusual and differs from the literature. Usually, the response time is shorter during the high water period (Larocque et al., 1998; Lee et al., 2006). The response time is less organised for the S3 borehole (Fig 5), this could be explained by the environment close to the borehole where there is runoff surfaces.

.

6. Discussion

The sliding cross-correlation between rainfall and piezometric level shows that the response time is shorter during the summer. Previous studies have also reported temporal variations in response time. Lee et al. (2006) showed that the response time is shorter during wet seasons in a chalk aquifer located in Southern England. They partially explain this evolution by seasonal variation in unsaturated zone thickness, with a major increase in time lag when the water table is below a critical depth. In this study, the relationship is reversed; the response time is shorter when the unsaturated zone is thicker (Fig 7). Therefore, the seasonal variation in response time is not a consequence of the decrease in distance between soil and the water table but is more likely due to a variability of the transfer velocities in the unsaturated zone.

Seasonal variability in the cross-correlation functions was observed by Larocque et al. (1998). These authors explained this evolution by the fact that during the high-water period, the water levels are higher, flooding some highly karstified fractures that transmit the pressure pulse more rapidly and directly. During the low-water period, these channels are unsaturated, and the pressure pulse is transmitted more slowly and homogenously in the saturated zone through deeper and narrower fractures. In the present study, the response time is slower during the low-water period (Fig. 7), but a variability in the transfer velocity depending on the saturation of conduits or fractures is conceivable.

The saturation of the unsaturated zone depends on rainfall characteristics. Precipitation data do not show a high seasonal variability in the monthly rainfall quantity (Fig. 5). Nevertheless, the rainfall intensity varies seasonally, with a higher intensity during the summer period (June, July and August) (Fig. 2), where the response time is shorter (Fig. 6). Therefore, we show a link between rainfall intensity and response time at most of the boreholes: when the rainfall intensity increases, the response time decreases (Fig. 8).

The results therefore show that the seasonal variability in the impulse response, and more precisely in the response time, is influenced by the seasonal variability of the input forcing (precipitation) and its effect on the hydrological process.

From the results, a conceptual model of the aquifer behaviour is drawn, particularly for the epikarst. The epikarst is the upper part of the infiltration zone where the permeability and the porosity are high in comparison to the rock underneath (Klimchouk, 2004). The variability of porosity and permeability induces the development of an epikarstic aquifer if the input flow, the efficient rainfall, is higher than the output flow, the water flow from the epikarst towards the transition and saturated zone (Mangin, 1975). There are two types of output flow:

(1) a “low” or “diffuse” flow by percolation to the base of the epikarst, characteristic of low permeability volumes and (2) the “fast” or “concentrated” flow by conduits or large fractures. The concentrated flow occurs when the epikarst is sufficiently saturated to allow lateral transfers that drive water in the conduits (Aquilina et al., 2005; Puech and Jeannin, 1997; Williams, 2008). Furthermore, Trček (2007) shows that the epikarst zone discharges dependent of the water storage volume and thus of the epikarst saturation; if the added volume of water is large, some of the water could be rapidly drained through large fractures into the epikarst conduit network. Thus, we can assume that the variability of the average water velocity in the infiltration zone depends on the epikarst saturation.

During the winter, and when a rainfall event occurs, it usually rains continuously during several days at a low intensity. Consequently, the difference between input and output flows of the epikarst is assumed to be small. It therefore takes more time to fill the epikarst aquifer, which induces a retardation of the "fast" transfer by conduits.

During the summer, the rainfall intensity is high and exceeds the output flow of the epikarst, which is rapidly saturated. Lateral flows occur rapidly in the epikarst and concentrate the transfer of water in preferential paths with a high permeability, inducing a “fast” transfer. In addition, the higher the rainfall intensity, the higher the piezometric level in the epikarstic aquifer. In the epikarst, the porosity and permeability increase exponentially towards the surface (Perrin et al., 2003). Thus, during high intensity rainfall events, some large fractures are flooded and rapidly transmit water towards the saturated zone.

The saturation in the epikarst could change depending on previous rainfall and air temperature. The variability in response time is larger during winter, corresponding to low rainfall intensities. This could be explained by the fact that if the rainfall event is less intense, the initial conditions of the epikarst have more impact on its saturation velocity and so on the response time (Fig. 9).

At most of the boreholes, the response time tends to reach a limit at high rainfall intensities (Fig. 9). This can be interpreted as the picture of the maximal transfer velocity (Table 3), probably due to maximum saturation of the epikarst. The minimum response time varies depending on the borehole, between 8 and 38 h (Table 3). The variability observed between the boreholes is most likely due to the heterogeneity of the epikarst.

7. Conclusions

In this study, we applied the sliding window cross-correlation method to analyse the seasonal variability of water transfer processes in a karst aquifer. We showed that its impulse response, and more particularly, its response time to rainfall, has a strong seasonality and gives information on the function of the unsaturated zone, which suggests the existence of an epikarst reservoir.

The karst aquifer is characterised by seasonal variability in response time, which is shorter during the summer. We explain this by variability in the input forcing, the rainfall intensity: an increase in rainfall intensity induces a decrease in response time. This evolution can be explained by variability in the epikarst saturation depending on rainfall intensity. During the summer, when rainfall intensity is higher, the epikarstic aquifer is quickly saturated, leading to fast and concentrated flows in the conduit porosities. In addition, high saturation of the epikarst induces the flooding of large conduits located in the upper zone of the epikarst that transmit the pressure pulse more rapidly and directly.

The conceptual model proposed, highlighted by seasonal variability in response time and hydrological processes, could be supported and validated by other methods, including geochemical or geophysical techniques.

Acknowledgements

The authors thank the French Atomic Agency (CEA) for access to the experimental site. Most of the experiments were completed with the enthusiastic and thoughtful collaboration of Patricia Gilbert, Yves Saulnier and Francois Alban. We thank A.J. Long and an anonymous reviewer for their helpful comments.

Figures:

Figure 1: *Description of the study area. The blue line represents the catchment limit, the grey area represents the urban area, the black line represents the faults and the black points represent the locations of the monitored boreholes.*

Figure 2*: Monthly averaged rainfall (histogram), monthly average air temperature (black line and dots) and monthly average rainfall intensity (gray line and dots), which is the average of rainfall intensity in mm/h without taking into account the intensities equal to zero, from meteorological data at Saint Martin du Mont (data Météo France) during the period 1992-2012.*

Figure 3: *Principle of the sliding cross-correlation method.*

(a) is the time series of rainfall and the piezometric level. Both time series are sliced with superposed windows. (b) is the cross-correlation function between rainfall and piezometric level on the first window. (c) and (d) are the cross-correlation functions for two following windows. For each cross-correlation function, the response time (RT) is determined. The time series of the response time is defined as (e).

Figure 4: *Rainfall and piezometric level time series for each borehole.*

Figure 5: *Time series of rainfall and response time for each borehole. The response time varies through the year. The dotted line (……) represents the absence of calculated response time due to a gap in the piezometric level data or a non-significant correlation coefficient of the cross-correlation function.*

Figure 6*: Monthly response time for the D1, D35, F7, A1 and C2 boreholes. The response time varies seasonally for these boreholes; the response time is lower during the summer period, from June to October.*

Figure 7*: Time series of response time at the F7 borehole calculated for each sliding cross-correlogram window and of the 3-month moving average of the piezometric level. The response time decreases when the thickness of the saturated zone increases.*

Figure 8: *Time series of intensity rainfall and response time at the F7 borehole. The rainfall and response time are anti-correlated, with a minimum response time when rainfall intensity is at a maximum.*

Figure 9*: Rainfall intensity versus response time for each studied borehole. For the A1, D35, F7, D1 and C2 boreholes, the response time decreases when the rainfall intensity increases, and the response time appears to tend towards a limit at high rainfall intensities.*

References:

Amraoui, F., Razack, M., Bouchaou, L., 2003. Turbidity dynamics in karstic systems. Example of Ribaa and Bittit springs in the Middle Atlas (Morocco). Hydrological Sciences Journal, 48(6): 971-984.

Andreo, B. et al., 2006. Climatic and hydrological variations during the last 117–166 years in the south of the Iberian Peninsula, from spectral and correlation analyses and continuous wavelet analyses. J. Hydrol., 324(1–4): 24-39.

Angelini, P., 1997. Correlation and spectral analysis of two hydrogeological systems in Central Italy. Hydrological Sciences Journal, 42(3): 425-438.

Aquilina, L., Ladouche, B., Dörfliger, N., 2005. Recharge processes in karstic systems investigated through the correlation of chemical and isotopic composition of rain and spring-waters. Appl. Geochem., 20(12): 2189-2206.

Atkinson, T.C., 1977. Diffuse flow and conduit flow in limestone terrain in the Mendip Hills, Somerset (Great Britain). J. Hydrol., 35(1–2): 93-110.

Bailly-Comte, V., Martin, J.B., Screaton, E.J., 2011. Time variant cross correlation to assess residence time of water and implication for hydraulics of a sink-rise karst system. Water Resour. Res., 47(5).

Bakalowicz, M., 2010. Karst et ressources en eau souterraine : un atout pour le développement des pays méditerranéens. Science et changements planétaires / Sécheresse, 21(4): 319-22.

Birk, S., Hergarten, S., 2010. Early recession behaviour of spring hydrographs. J. Hydrol., 387(1–2): 24-32.

Bouchaou, L., Mangin, A., Chauve, P., 2002. Turbidity mechanism of water from a karstic spring: example of the Ain Asserdoune spring (Beni Mellal Atlas, Morocco). J. Hydrol., 265(1–4): 34-42.

Box, G.E.P., Jenkins, G.M., Reinsel, G.C., 1994. Time Series Analysis: Forecasting and Control. Prentice Hall Inc. Englewood Cliffs, NJ, USA.

Diggle, P.D., 1990. Times series: A biostatistical introduction. Oxford Statistical Science Series. Oxford Science Publications.

Dreybrodt, W., 1996. Principles of Early Development of Karst Conduits Under Natural and Man-Made Conditions Revealed by Mathematical Analysis of Numerical Models. Water Resour. Res., 32(9): 2923-2935.

Dreybrodt, W., Gabrovsek, F., Romanov, D., 2005. Processes of Speleogenesis: A modeling approach. Karst Research Institute, ZRC SAZU, Postojna, Slovenia.

Drogue, C., 1974. Structure de certains aquifères karstiques d'après les résultats de travaux de forage. CR Acad Sci Paris,série IIII, 278: 2621–2624.

Eisenlohr, L., Bouzelboudjen, M., Király, L., Yvan, R., 1997. Numerical versus statistical modelling of natural response of a karst hydrogeological system. J. Hydrol., 202(1–4): 244-262.

Emblanch, C., Zuppi, G.M., Mudry, J., Blavoux, B., Batiot, C., 2003. Carbon 13 of TDIC to quantify the role of the unsaturated zone: the example of the Vaucluse karst systems (Southeastern France). J. Hydrol., 279(1–4): 262-274.

Fleury, P., Plagnes, V., Bakalowicz, M., 2007. Modelling of the functioning of karst aquifers with a reservoir model: Application to Fontaine de Vaucluse (South of France). J. Hydrol., 345(1–2): 38-49.

Geyer, T., Birk, S., Liedl, R., Sauter, M., 2008. Quantification of temporal distribution of recharge in karst systems from spring hydrographs. J. Hydrol., 348(3–4): 452-463.

Goldscheider, N., Meiman, J., Pronk, M., Smart, C.C., 2008. Tracer tests in karst hydrogeology and speleology. International Journal of Speleology, 37: 27-40.

Hanin, G., 2010. Contrôles structural et hydrogéologique sur la dynamique d'un champ captant en contexte crayeux karstique et sa sensibilité aux variations du signal climatique :Implications en matière de vulnérabilité de la ressource. Thèse de doctorat Thesis, Université de Rouen, 306 pp.

Jacob, T. et al., 2008. Absolute gravity monitoring of water storage variation in a karst aquifer on the larzac plateau (Southern France). J. Hydrol., 359(1–2): 105-117.

Jenkins, G.M., Watts, D.G., 1968. Spectral Analysis and its Applications. Holden Day, San Francisco, CA, 525 pp.

Jukić, D., Denić-Jukić, V., 2004. A frequency domain approach to groundwater recharge estimation in karst. J. Hydrol., 289(1–4): 95-110.

Jukić, D., Denić-Jukić, V., 2009. Groundwater balance estimation in karst by using a conceptual rainfall–runoff model. J. Hydrol., 373(3–4): 302-315.

Jukić, D., Denić-Jukić, V., 2011. Partial spectral analysis of hydrological time series. J. Hydrol., 400(1–2): 223-233.

Käss, W., 1998. Tracing Technique in Geohydrology. Balkema, Rotterdam, 600 pp.

Klimchouk, A., 2004. Towards defining, delimiting and classifying epikarst: Its origin, processes and variants of geomorphic evolution. Speleogenesis and Evolution of Karst Aquifers, 2(1).

Kogovsek, J., Petric, M., 2003. Tracing test as a tool for the estimation of possible impacts of human activities on karst water-examples from Slovenia. Materials and Geoenvironment, 50(1): 161-164.

Kovács, A., Perrochet, P., 2008. A quantitative approach to spring hydrograph decomposition. J. Hydrol., 352(1–2): 16-29.

Labat, D., Ababou, R., Mangin, A., 2000. Rainfall–runoff relations for karstic springs. Part II: continuous wavelet and discrete orthogonal multiresolution analyses. J. Hydrol., 238(3–4): 149-178.

Larocque, M., 1997. Intégration d'approches quantitatives de caractérisation et de simulation des aquifères calcaires fissurés - application à l'aquifère karstique de la Rochefoucauld (Charentes, France). Thèse de doctorat Thesis, Université de Poitier.

Larocque, M., Mangin, A., Razck, M., Banton, O., 1998. Contribution of correlation and spectral analyses to the regional study of a large karst aquifer (Charente, France). J. Hydrol., 205: 217-231.

Lee, L.J.E., Lawrence, D.S.L., Price, M., 2006. Analysis of water-level response to rainfall and implications for recharge pathways in the Chalk aquifer, SE England. J. Hydrol., 330(3–4): 604-620.

Mangin, A., 1975. Contribution à l'étude hydrodynamique des aquifères karstiques. Thèse de Doctorat d'Etat, Université de Dijon Thesis.

Mangin, A., 1984. Pour une meilleure connaissance des systèmes hydrologiques à partir des analyses corrélatoire et spectrale. J. Hydrol., 67(1–4): 25-43.

Massei, N. et al., 2006. Investigating transport properties and turbidity dynamics of a karst aquifer using correlation, spectral, and wavelet analyses. J. Hydrol., 329(1–2): 244-257.

Mathevet, T., Lepiller, M., Mangin, A., 2004. Application of time-series analyses to the hydrological functioning of an Alpine karstic system: the case of Bange-L'Eau-Morte. Hydrol. Earth. Syst. Sc., 8(6): 1051-1064.

McConnell, C.L., 1993. Double porosity well testing in the fractured carbonate rocks of the Ozarks. Groundwater, 31 (1): 75-83.

Milanovic, P.T., 1981. Karst Hydrogeology. Water Resources Pubs, Colorado: 434 pp.

Mudry, J., 1990. Les courbes flux chimique-debit et le fonctionnement des aquiferes karstiques. J. Hydrol., 120(1–4): 283-294.

Panagopoulos, G., Lambrakis, N., 2006. The contribution of time series analysis to the study of the hydrodynamic characteristics of the karst systems: Application on two typical karst aquifers of Greece (Trifilia, Almyros Crete). J. Hydrol., 329: 368-376.

Perrin, J., Jeannin, P.-Y., Zwahlen, F., 2003. Epikarst storage in a karst aquifer: a conceptual model based on isotopic data, Milandre test site, Switzerland. J. Hydrol., 279(1–4): 106-124.

Puech, V., Jeannin, P.-Y., 1997. Contribution à la compréhension du fonctionnement hydraulique de l'épikarst; expériences d'arrosage sur le site de Bure (Jura, Suisse). Proceedings of the 12th International Congress of Speleology, 1.

Pulido-Bosch, A., Padilla, A., Dimitrov, D., Machkova, M., 1995. The discharge variability of some karst springs in Bulgaria studied by time series analysis. Hydrological Sciences Journal, 40(4): 517-532.

Rahnemaei, M., Zare, M., Nematollahi, A.R., Sedghi, H., 2005. Application of spectral analysis of daily water level and spring discharge hydrographs data for comparing physical characteristics of karstic aquifers. J. Hydrol., 311(1–4): 106-116.

Scanlon, B.R., Mace, R.E., Barrett, M.E., Smith, B., 2003. Can we simulate regional groundwater flow in a karst system using equivalent porous media models? Case study, Barton Springs Edwards aquifer, USA. J. Hydrol., 276(1–4): 137-158.

Shevenell, L., 1996. Analysis of well hydrographs in a karst aquifer: estimates of specific yields and continuum transmissivities. J. Hydrol., 174(3–4): 331-355.

Smart, C.C., 1988. Artificial Tracer Techniques for the Determination of the Structure of Conduit Aquifers. Ground Water, 26(4): 445-453.

Thrailkill, J., 1988. Drawdown interval analysis: A method of determining the parameters of shallow conduit flow carbonate aquifers from pumping tests. Water Resour. Res., 24(8): 1423-1428.

Trček, B., 2007. How can the epikarst zone influence the karst aquifer hydraulic behaviour? Environ Geol, 51(5): 761-765.

Tritz, S., Guinot, V., Jourde, H., 2011. Modelling the behaviour of a karst system catchment using non-linear hysteretic conceptual model. J. Hydrol., 397(3–4): 250-262.

Walliser, B., 1977. Systèmes et modèles Seuil, Paris, France.

White, W.B., 1969. Conceptual Models for Carbonate Aquifers. Ground Water, 7(3): 15-21.

White, W.B., 2002. Karst hydrology: recent developments and open questions. Eng. Geol., 65: 85–105.

Williams, P., 2008. The role of the epikarst in karst and cave hydrogeology: a review. International Journal of Speleology, 37(1): 1-10.

Tables:

Table 1: Key characteristics of monitored boreholes. The unsaturated zone was measured at the same date for each borehole during a low water level (July 2010).

Borehole	Dominant land use	Wellhead altitude (m NGF)	Unsaturated zone thickness (m)
A1	Industrial land use	496.9	69.4
C2	Forest	472.0	38.1
D1	Forest	367.6	5.0
D35	Forest	429.5	31.6
F7	Forest	469.4	52.5
S3	Industrial land use	500.4	33.7

Table 2: Results of the application of the sliding cross-correlogram between rainfall and the piezometric level: characteristics of response times and coefficient correlations of the time series.

Borehole	Maximum response time (h)	Minimum response time (h)	Mean response time (h)	Maximum coefficient correlation	Minimum coefficient correlation
A1	42	5	15.48	0.513	0.071
C2	107	26	49.34	0.331	0.061
D1	118	28	52.38	0.403	0.046
D35	140	9	40.43	0.463	0.066
F7	107	20	38.90	0.398	0.055
S3	52	12	23.58	0.449	0.068

Table 3: Values of the minimum response time determined from the asymptote described by the relationship between rainfall intensity and response time (fig. 9).

Borehole	Minimum response time defined from the asymptote (h)
A1	8
C2	34
D1	38
D35	13
F7	21

Figure1

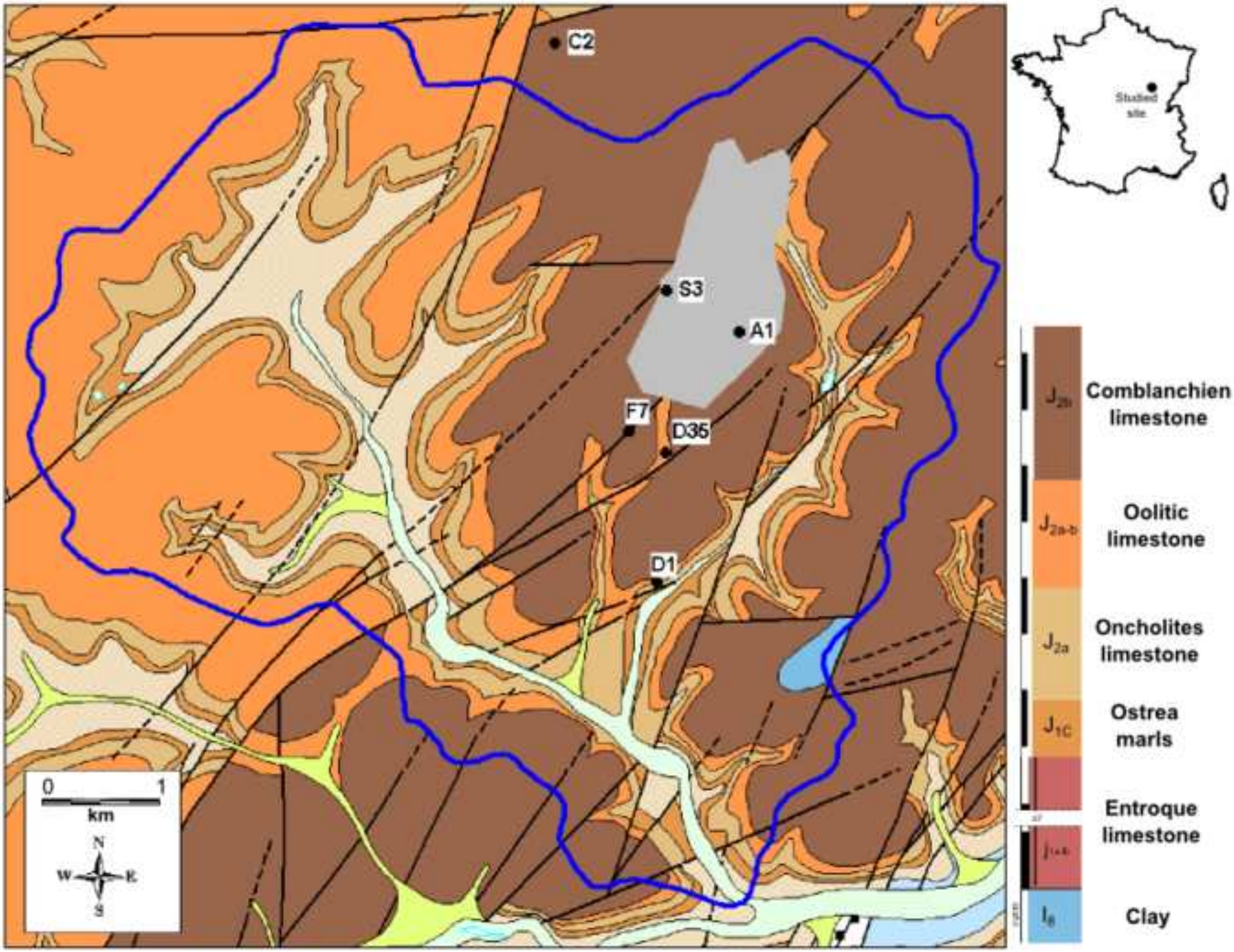
C2
S3
A1
F7
D35
D1
0
1
km
N
W
E
S
Studied site
J2b
Comblanchien limestone
J2a-b
Oolitic limestone
J2a
Oncholites limestone
J1C
Ostrea marls
Entroque limestone
I6
Clay

Figure2

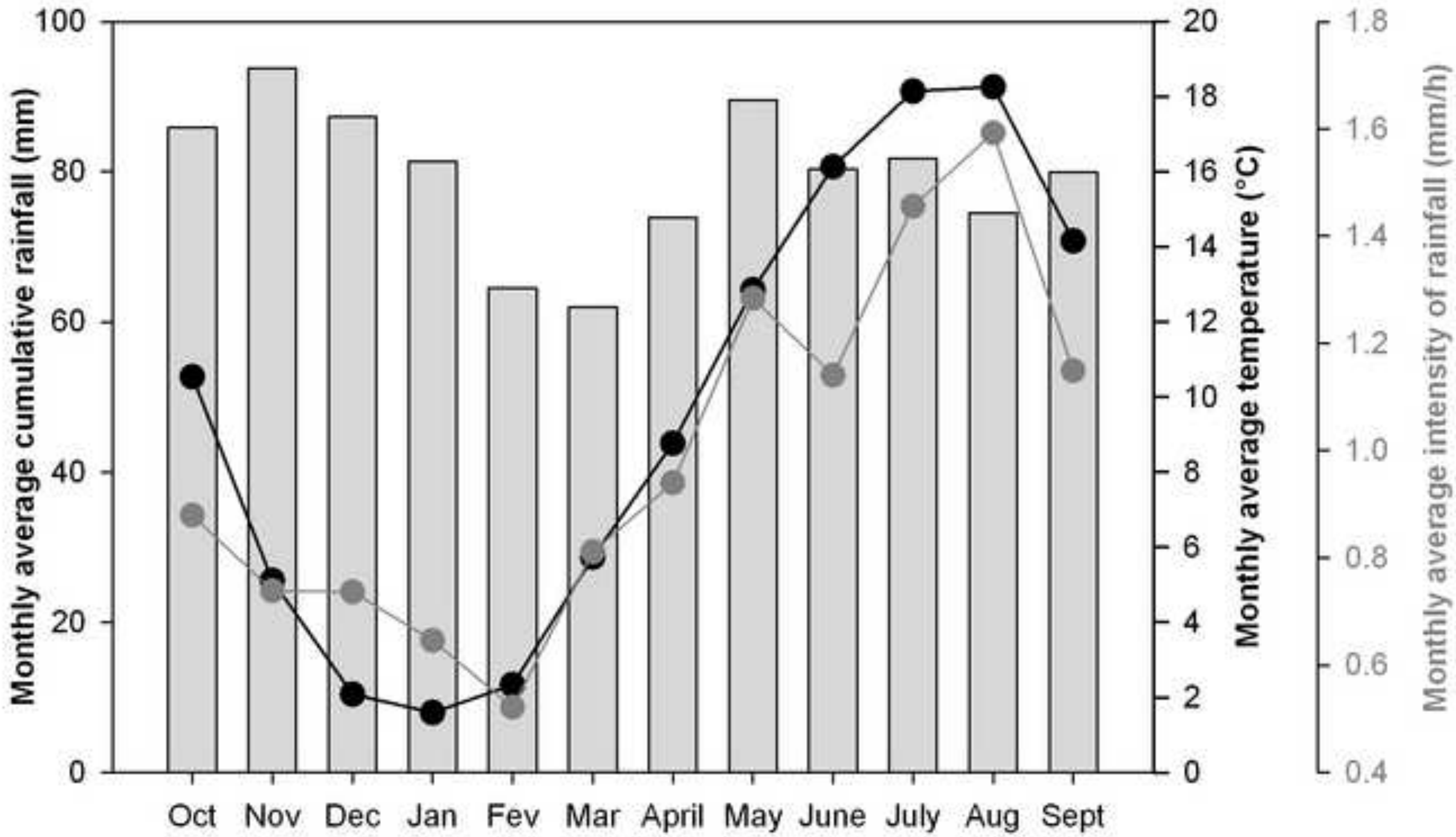
Monthly average cumulative rainfall (mm)
Monthly average temperature (°C)
Monthly average intensity of rainfall (mm/h)
100
80
60
40
20
0
20
18
16
14
12
10
8
6
4
2
0
1.8
1.6
1.4
1.2
1.0
0.8
0.6
0.4
Oct
Nov
Dec
Jan
Fev
Mar
April
May
June
July
Aug
Sept

Figure 3

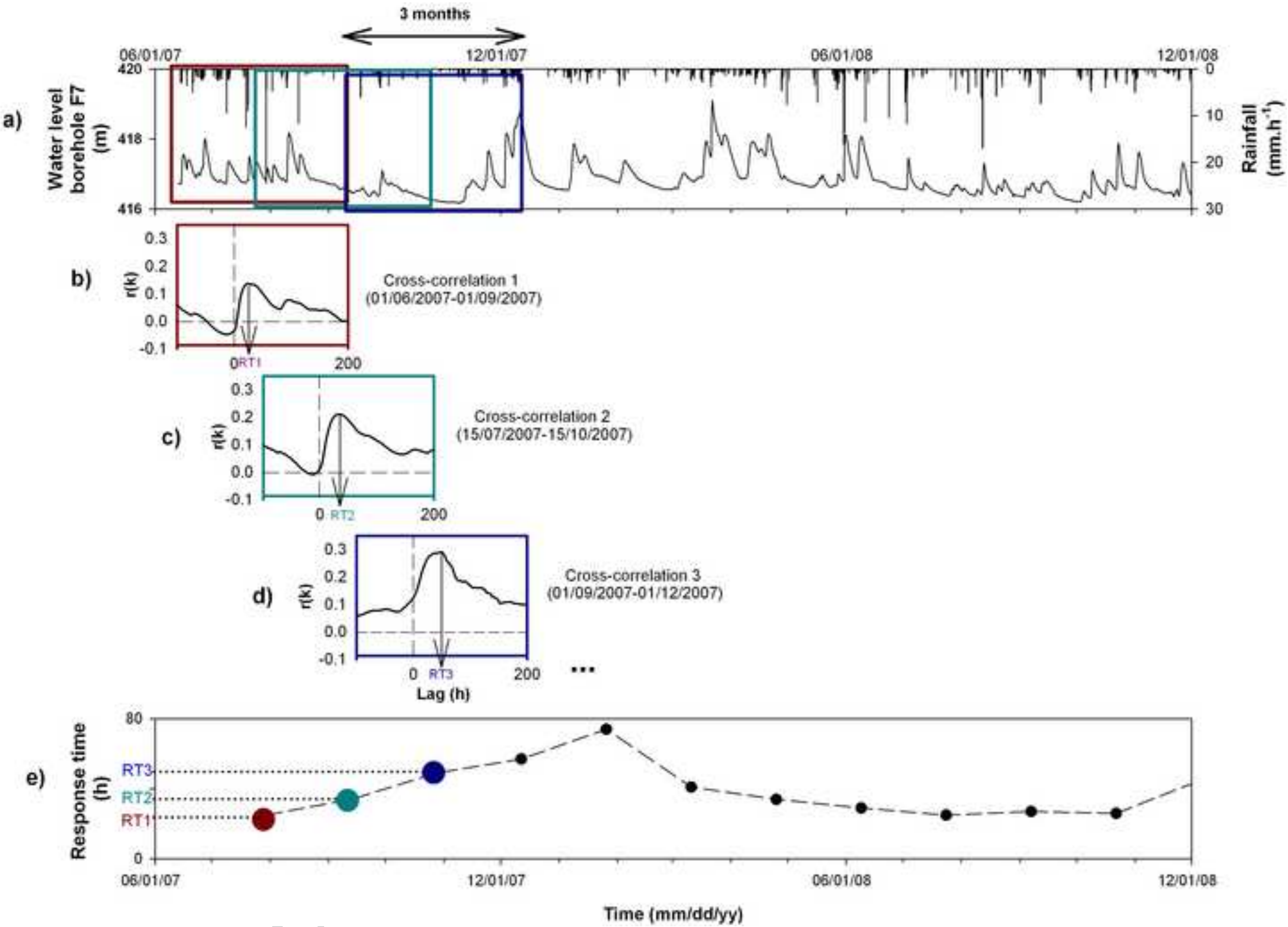
3 months
06/01/07
12/01/07
06/01/08
12/01/08
a)
Water level borehole F7 (m)
Rainfall (mm.h-1)
b)
r(k)
Cross-correlation 1
(01/06/2007-01/09/2007)
RT1
c)
Cross-correlation 2
(15/07/2007-15/10/2007)
RT2
d)
Cross-correlation 3
(01/09/2007-01/12/2007)
RT3
Lag (h)
e)
Response time (h)
Time (mm/dd/yy)

Figure 4

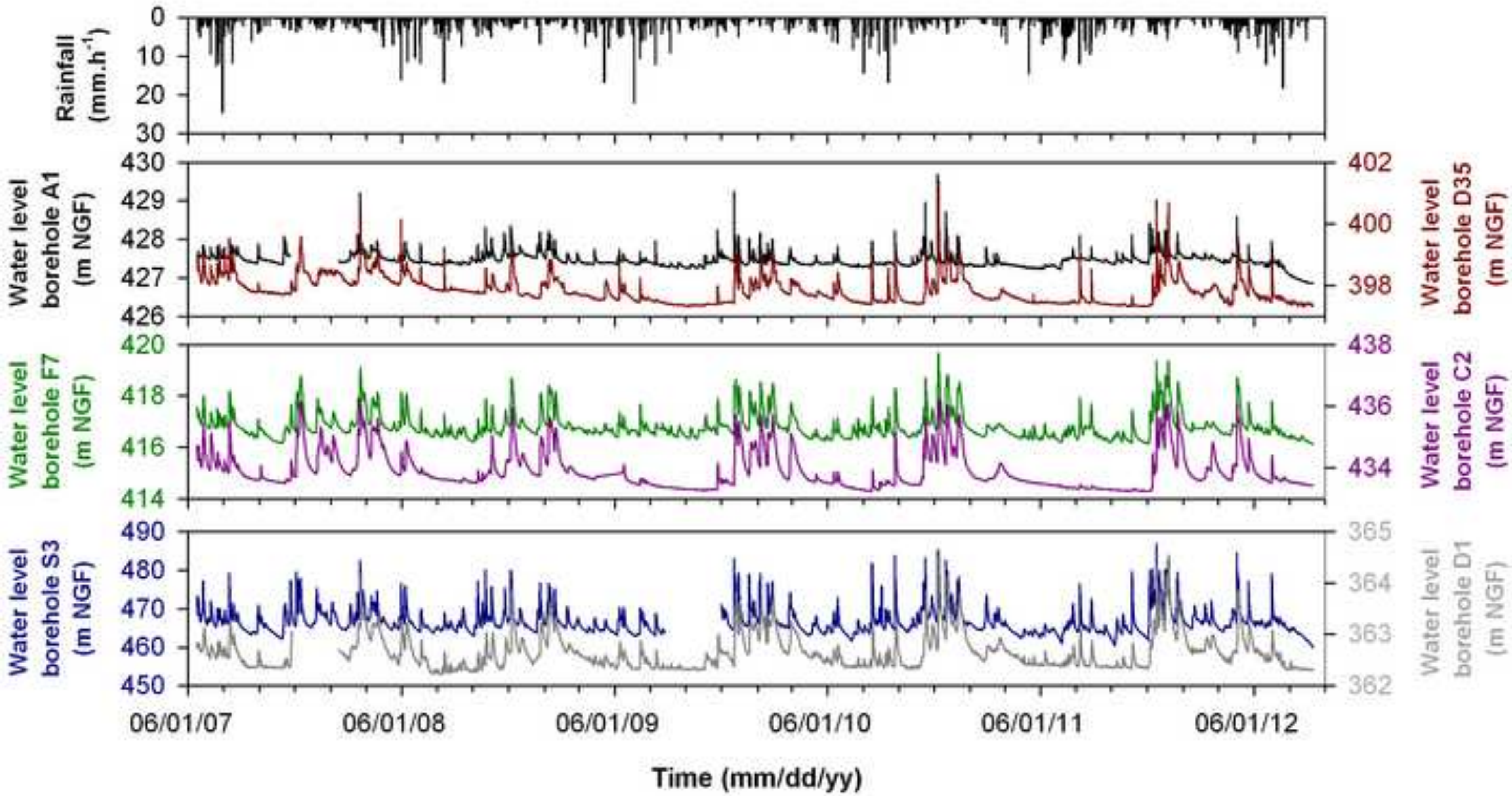
Rainfall (mm.h^{-1})
0
10
20
30
Water level borehole A1 (m NGF)
430
429
428
427
426
Water level borehole D35 (m NGF)
402
400
398
Water level borehole F7 (m NGF)
420
418
416
414
Water level borehole C2 (m NGF)
438
436
434
Water level borehole S3 (m NGF)
490
480
470
460
450
Water level borehole D1 (m NGF)
365
364
363
362
06/01/07
06/01/08
06/01/09
06/01/10
06/01/11
06/01/12
Time (mm/dd/yy)

Figure 5

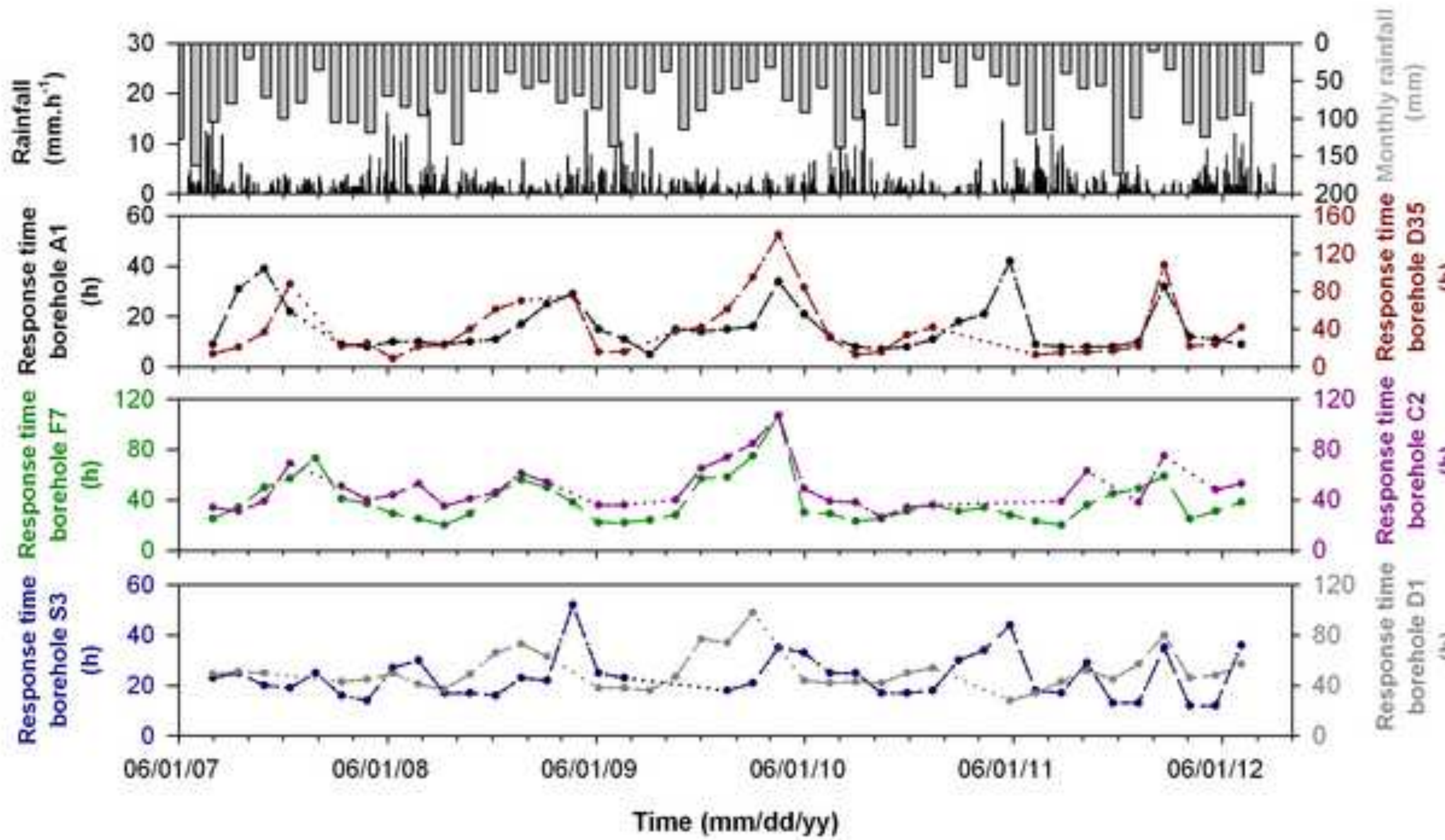
Rainfall (mm.h-1)
Monthly rainfall (mm)
Response time borehole A1 (h)
Response time borehole D35 (h)
Response time borehole F7 (h)
Response time borehole C2 (h)
Response time borehole S3 (h)
Response time borehole D1 (h)
06/01/07
06/01/08
06/01/09
06/01/10
06/01/11
06/01/12
Time (mm/dd/yy)

Figure 6

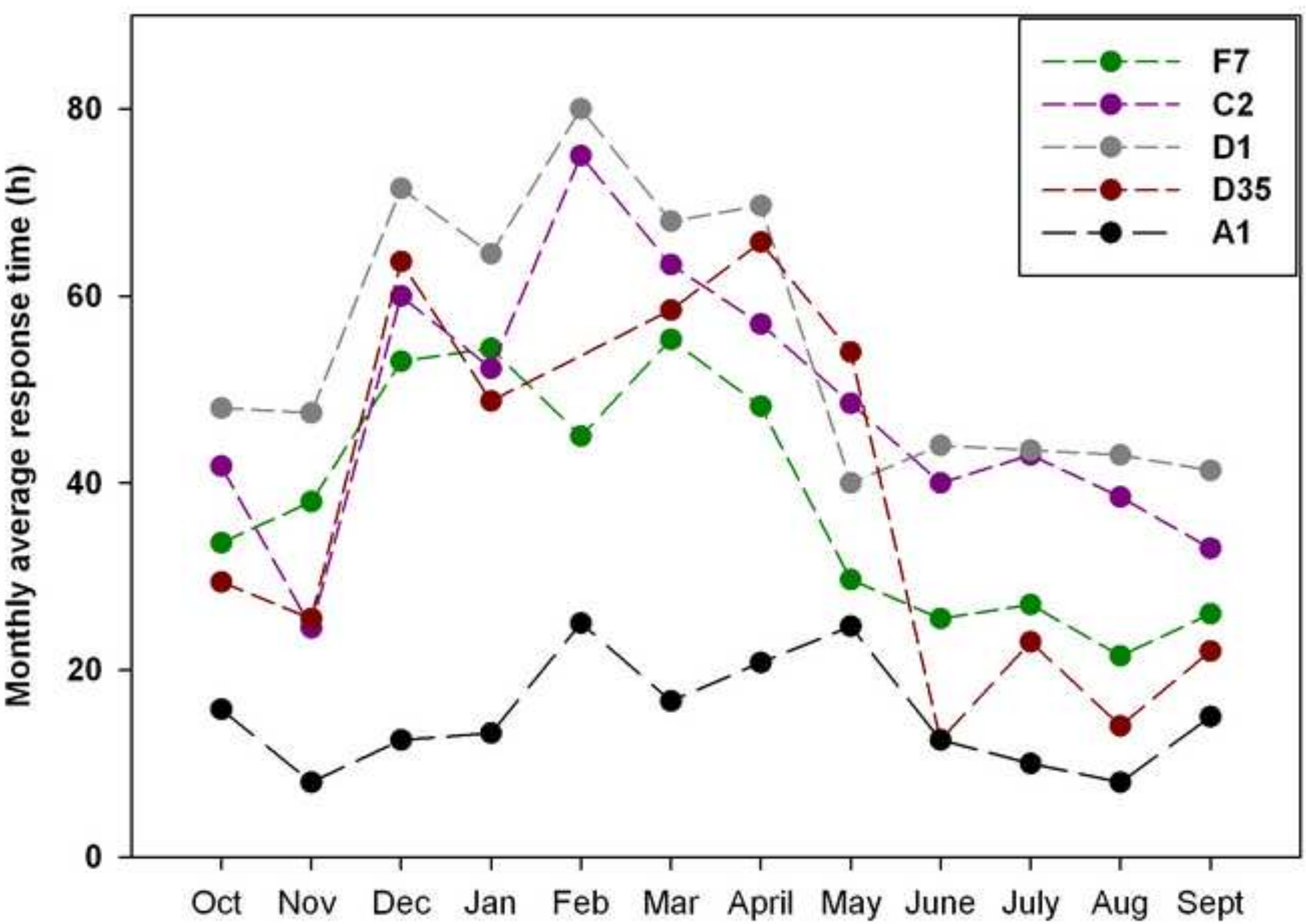
F7
C2
D1
D35
A1
Monthly average response time (h)
0
20
40
60
80
Oct
Nov
Dec
Jan
Feb
Mar
April
May
June
July
Aug
Sept

Figure 7

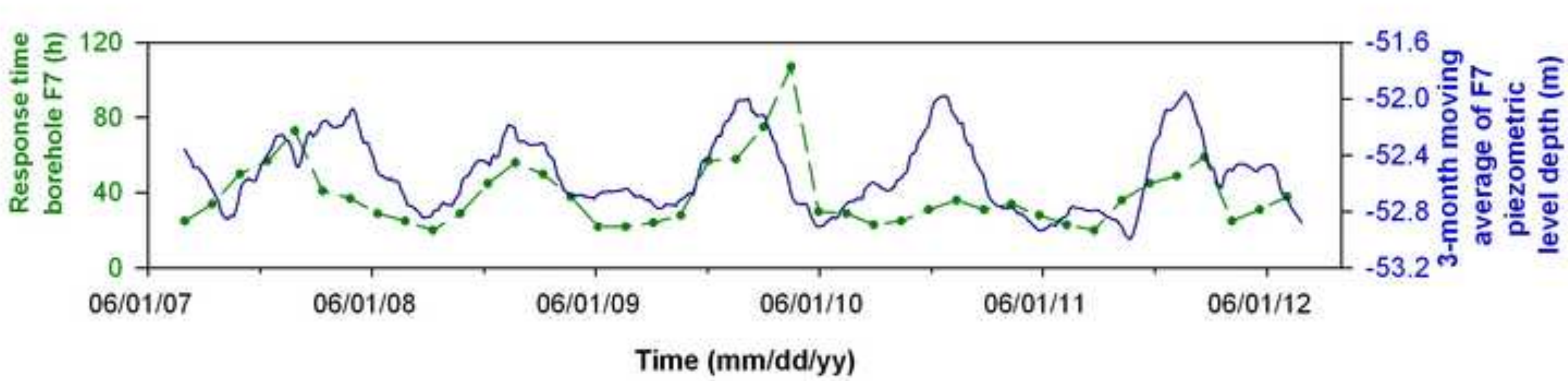

Response time borehole F7 (h)
120
80
40
0
-51.6
-52.0
-52.4
-52.8
-53.2
3-month moving average of F7 piezometric level depth (m)
06/01/07
06/01/08
06/01/09
06/01/10
06/01/11
06/01/12
Time (mm/dd/yy)

Figure 8

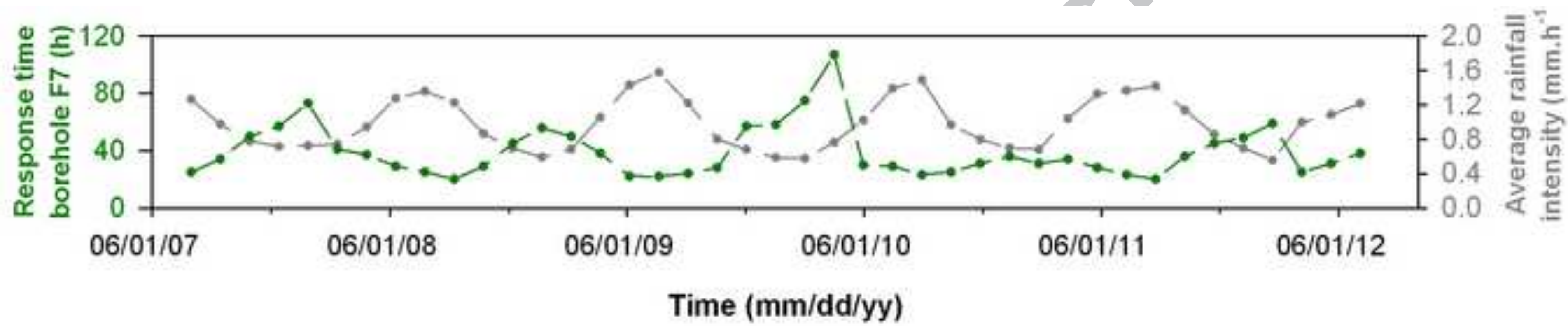

Response time borehole F7 (h)
120
80
40
0
Average rainfall intensity (mm.h^{-1})
2.0
1.6
1.2
0.8
0.4
0.0
06/01/07
06/01/08
06/01/09
06/01/10
06/01/11
06/01/12
Time (mm/dd/yy)

Figure 9

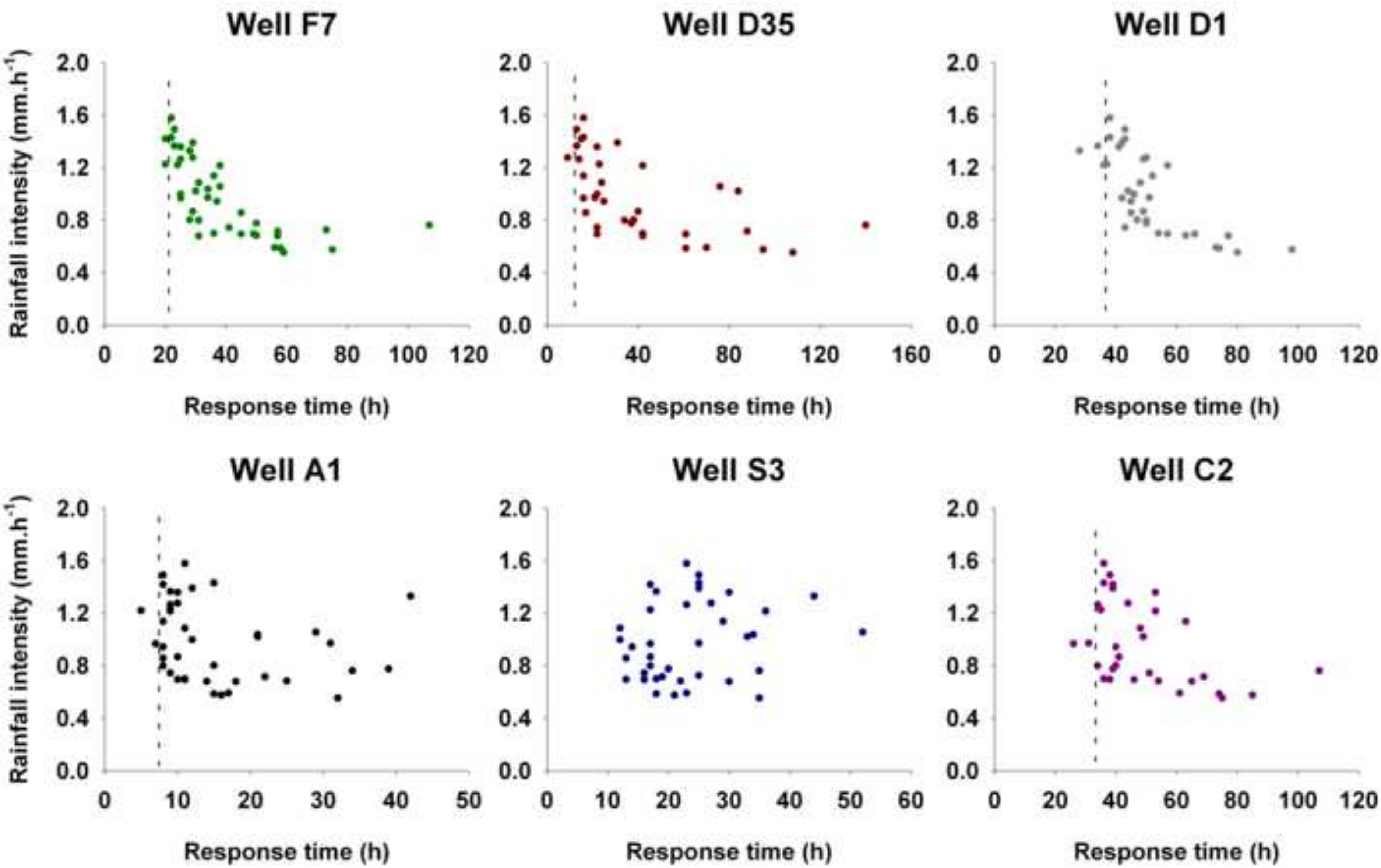

Well F7
Well D35
Well D1
Well A1
Well S3
Well C2
Rainfall intensity (mm.h^{-1})
Response time (h)

Highlights:

- Sliding window cross-correlation highlights the karst response time seasonality.
- The response time varies seasonally with an uncommon rise during winter.
- The response time depends on the rainfall intensity.
- The rainfall intensity modifies the hydrological process in the epikarstic zone.